



Published in final edited form as:

*Mol Ther.* 2008 August ; 16(8): 1459–1466. doi:10.1038/mt.2008.119.

## Targeting of the CNS in MPS-IH Using a Nonviral Transferrin- $\alpha$ -L-Iduronidase Fusion Gene Product

Mark J Osborn<sup>1,2</sup>, Ron T McElmurry<sup>1,2</sup>, Brandon Peacock<sup>1,2</sup>, Jakub Tolar<sup>1,2</sup>, and Bruce R Blazar<sup>1,2</sup>

<sup>1</sup>University of Minnesota Cancer Center, Minneapolis, Minnesota, USA

<sup>2</sup>Department of Pediatrics, Division of Bone Marrow Transplant, University of Minnesota, Minneapolis, Minnesota, USA

### Abstract

Mucopolysaccharidosis type I (Hurler syndrome) is caused by a deficiency of the enzyme  $\alpha$ -L-iduronidase (IDUA), and is characterized by widespread lysosomal glycosaminoglycan (GAG) accumulation. Successful treatment of central nervous system (CNS) diseases is limited by the presence of the blood–brain barrier, which prevents penetration of the therapeutic enzyme. Given that the brain capillary endothelial cells that form this barrier express high levels of the transferrin receptor (TfR), we hypothesized that the coupling of IDUA to transferrin (Tf) would facilitate IDUA delivery to the CNS. A plasmid bearing a fusion gene consisting of Tf and IDUA was constructed which, when delivered *in vivo*, resulted in the production of high levels of an enzymatically active protein that was transported into the CNS by TfR-mediated endocytosis. Short-term treatment resulted in a decrease in GAGs in the cerebellum of mucopolysaccharidosis type I (MPS I) mice. This approach, therefore, represents a potential strategy for the delivery of therapeutic enzyme to the CNS.

### INTRODUCTION

The mucopolysaccharidoses (MPSs) are inherited lysosomal hydrolase enzymopathies resulting in defects in the stepwise catabolism of glycosaminoglycans (GAGs).<sup>1</sup> MPS I (Hurler syndrome) is characterized by a deficiency of  $\alpha$ -L-iduronidase (IDUA; EC 3.2.1.76) resulting in lysosomal accumulation of heparan and dermatan sulfate with progressive cellular and multiorgan dysfunction.<sup>2</sup> The central nervous system (CNS) pathological manifestations include progressive intellectual decline, spinal cord compression, and communicating hydrocephalus.<sup>3–8</sup>

The available treatments for MPS I are either allogeneic bone marrow transplantation or IDUA enzyme replacement therapy, both of which provide an extracellular source of enzyme that can be taken up through the mannose 6-phosphate receptor (M6PR) that is present on most cells.<sup>9–11</sup> If MPS patients receive transplants before the age of 2, the donor-derived microglial cell engraftment into the CNS can be protected against irreversible neuropathology.<sup>12</sup> However, in addition to the side effects of allogeneic bone marrow transplantation, including both morbidity and mortality caused by the conditioning regimen and the immune responses between the donor and the host, many patients continue to experience a decline in their intellectual abilities prior to stabilization, and will still require special educational needs.<sup>9</sup> Enzyme replacement therapy

**Correspondence:** Bruce R. Blazar, University of Minnesota, 420 Delaware Street SE, MMC 109, Minneapolis, Minnesota 55455. E-mail: blaza001@umn.edu.

The last two authors contributed equally to this work.

with recombinant human IDUA (Aldurazyme®/Laronidase) shows therapeutic benefit in non-CNS organs but appears to have limited efficacy in correcting CNS pathology, apparently because of its limited ability to cross the blood–brain barrier (BBB).<sup>13–15</sup> It is desirable, therefore, to devise strategies that are alternatives to bone marrow transplantation or enzyme replacement therapy, and that are capable of more efficiently delivering IDUA to the brain while minimizing adverse side effects.

Strategies for breaching the BBB include the use of osmotic agents to disrupt the barrier and carrier proteins to deliver cargo across the intact BBB through transcytosis.<sup>16–18</sup> One such study involved the use of the rat 8D3 monoclonal antibody to the transferrin receptor (TfR) as a molecular Trojan horse to deliver a bacterial enzymatic reporter,  $\beta$ -galactosidase, across the BBB.<sup>19</sup> This protein-based system requires chemical conjugation of the enzyme to the antibody. Except where the antibody used for CNS targeting is fully humanized, immune responses to the antibody moiety itself may occur after the administration of repeated injections of the protein–enzyme complex (required for maintaining sufficiently high CNS enzyme levels for curative intent). Therefore, we sought to determine whether a DNA-based approach using a Tf–IDUA fusion gene would be capable of delivering functional IDUA enzyme to the CNS. We demonstrate a strategy utilizing the liver as a depot organ for continuous production of a Tf–IDUA fusion protein that can gain access to the CNS in adult MPS I mice.

## RESULTS

### Plasmid design, fusion gene activity, cellular localization, and uptake *in vitro*

A cytomegalovirus promoter–regulated plasmid was generated, wherein full-length murine Tf cDNA was fused to the human IDUA cDNA devoid of its signal sequence. A 6-amino-acid linker was used as a spacer between the two genes to provide separation, facilitating the proper folding of each protein. The design of the plasmid, termed Tf-ID, is shown in Figure 1a. A full-length human IDUA cDNA (termed Mono-ID) under the control of the cytomegalovirus promoter was generated for comparison (Figure 1a). Equimolar DNA amounts of the Tf-ID or Mono-ID plasmids were transfected into NIH-3T3 cells, and each showed specificity toward an artificial substrate (Figure 1b). The Mono-ID-transfected cells showed high activity levels in the cellular lysate, with Tf-ID showing less intracellular enzyme.

The normal cellular location of IDUA is the lysosome, the organelle that accumulates partially degraded GAGs in the MPSs. In order to ensure that the fusion protein was localized to the lysosome, we generated a plasmid in which the DsRed monomer was fused to the Tf-ID (Figure 1a) that was transfected into Chinese hamster ovary cells (Figure 1c). Subsequently, a lysosomal tracking dye was added (Figure 1d), and we observed co-localization of the two signals (Figure 1e).

In order to determine whether the inclusion of the Tf moiety resulted in TfR-mediated uptake, equal enzymatic activity amounts of recombinant Tf-ID or IDUA were incubated with 3T3 cells in the presence or absence of free Tf (fTf) or free M6P. The uptake of recombinant Tf-ID was completely inhibited by fTf and partially inhibited by M6P (Figure 2a). In contrast, recombinant human IDUA uptake was completely inhibited by free M6P but was not inhibited by the addition of fTf (Figure 2a).

In order to determine whether generation of the fusion protein had an effect on IDUA enzymatic activity, we compared Mono-ID protein and Tf-ID protein at a ratio of 1:1. The results showed a slight decrease in enzymatic activity of the fusion protein as compared to the native enzyme (Figure 2b). In order to determine whether the specificity for the TfR was altered in the Tf-ID fusion, we compared its ability to inhibit uptake of a Tf–fluorescein isothiocyanate molecule to that of native Tf. On a molar basis, native Tf protein and Tf-ID fusion protein showed near-

similar abilities to inhibit uptake of Tf-fluorescein isothiocyanate into 3T3 cells (Figure 2c). Taken together, the results shown in Figure 1 and Figure 2 confirm that Tf-ID (i) retains enzymatic activity, (ii) maintains specificity for, and is taken up by, the TfR (and to a lesser extent through the M6PR) and, importantly, (iii) is routed to the lysosome.

### Fusion gene activity and uptake *in vivo*

We have reported earlier that human IDUA protein could be detected in the serum after the hydrodynamic delivery of an IDUA-containing plasmid in mice.<sup>20</sup> In order to characterize Tf-ID *in vivo*, nonobese diabetic-severe combined immunodeficiency (NOD-SCID) mice were injected with Tf-ID plasmid DNA by hydrodynamic tail vein injection.<sup>21</sup> At 48 hours, serum was harvested and western blotting was performed using an anti-Tf antibody or anti-human IDUA antibody that can detect human, but not murine, IDUA protein. Full-length Tf-ID (~150 kd) was detectable using both antibodies (Figure 3a). We next compared plasmids bearing Tf-ID, Mono-ID, or a version of the fusion gene lacking the Tf signal sequence (deltaSS Tf-ID; Figure 1a). A significant increase in IDUA enzyme activity was seen in the sera of Tf-ID-treated animals as compared to Mono-ID- and deltaSS Tf-ID-treated animals (Figure 3b). Importantly, IDUA activity in the brain was also significantly increased in mice that were given Tf-ID as compared to Mono-ID-injected mice (Figure 3b). Removal of the signal sequence (deltaSS Tf-ID-treated animals) resulted in a near-complete absence of enzyme in the serum and brain. These results show that the Tf-ID signal sequence is required for efficient secretion and activity of the full-length fusion protein, which was detectable in the lysates of brain tissue.

We considered the possibility that, in addition to bona fide TfR-mediated uptake of Tf-ID, brain enzyme activity may also be caused by local enzyme production from plasmid DNA (present in the brain as a result of intravenous injection), or by the higher levels of serum enzyme achieved in Tf-ID mice. This scenario was considered because of earlier observations that administration of extremely high levels of recombinant enzyme were associated with delivery to the CNS in MPS VII mice.<sup>22</sup> In order to determine whether the former had occurred, we assessed the biodistribution of plasmid DNA after hydrodynamic delivery by injecting a vector expressing a nonsecreted protein, firefly luciferase, at fivefold (250 µg) the concentration of the Tf-ID plasmid. *In vivo* bioluminescent Xenogen imaging performed 48 hours after the injection showed luciferase expression localized to the liver (Figure 4a). The individual organs were removed and subjected to *in vitro* luciferase assays. The results showed that ~99% of the luciferase activity was confined to the liver, and no detectable luciferase activity was present in the brain (Figure 4b). From these data we conclude that, after hydrodynamic tail vein injection, plasmid DNA is restricted to non-CNS tissues; therefore, brain IDUA enzyme activity in Tf-ID-injected mice cannot be because of local Tf-ID plasmid within the brain.

In order to determine whether the enzyme detected in the brain lysates (shown in Figure 3) was caused by enzyme present in the serum acting as a contaminant, or whether high enzyme levels alone were sufficient to allow for entry into the CNS, we used the brain capillary depletion method, removing the capillaries of the brain and leaving only parenchymal tissue.<sup>23</sup> Our initial tests using this method in mice treated with equimolar amounts of Tf-ID or Mono-ID revealed IDUA presence only in the brains of Tf-ID-treated mice (data not shown). However, the disparity in the serum levels between the Tf-ID- and Mono-ID-treated mice was the same as shown in Figure 3b. Therefore, we varied the doses of plasmid in an attempt to achieve equal serum levels of each enzyme. However, even when the Tf-ID injected was 25 times less than Mono-ID, the serum enzyme levels in Tf-ID-treated animals were still almost twofold higher than in Mono-ID-treated animals (data not shown). In order to create a scenario wherein serum IDUA levels would be similar between treatment groups, we injected a large bolus of recombinant IDUA protein (Aldurazyme) at a dose equivalent to 10 times the amount given

to human patients,<sup>24</sup> and performed the brain capillary depletion method 1 hour after injection. Aldurazyme injection resulted in statistically higher serum levels of nonfusion protein as compared to low-dose Tf-ID-treated animals (Figure 4c). However, brain enzyme levels were statistically significantly higher in Tf-ID plasmid animals, showing that high levels of enzyme present in the lumen of vessels can be removed and does not “contaminate” the brain parenchymal fraction. These studies served to validate the brain capillary depletion assay, and indicated that Tf-ID was present in the brain parenchyma. However, the results did not indicate whether Tf-ID was present in the brain because of transcytosis of the BBB mediated by the TfR, or whether simply because of nonspecific entrance into the CNS as a result of high serum enzyme levels. Therefore, in order to elucidate the mechanism of CNS uptake *in vivo*, Tf-ID plasmid was administered to NOD-SCID mice, alone or along with supplemental free Tf protein to block endogenous TfR. In the presence of prior TfR blockade, the higher brain IDUA enzyme levels that had been found in Tf-ID plasmid-injected mice were reduced to the levels seen in noninjected controls (Figure 4d). Importantly, serum IDUA levels in animals receiving Tf-ID did not differ depending on whether it was administered alone or in conjunction with free Tf (Figure 4e). Taken together, our results show higher levels of brain IDUA in Tf-ID-treated mice as compared to Mono-ID-treated mice, and provide strong evidence that Tf-ID protein in the brain is attributable to TfR-mediated uptake of the enzyme from non-CNS organs (primarily from the liver).

### Tf-ID biodistribution, immunofluorescence, and pathology in MPS I mice

Studies in NOD-SCID mice revealed both Tf-ID and Mono-ID in the serum, and only Tf-ID in brain lysates. However, these recipients lack GAG accumulation, the substrate targeted by this approach. Because organomegaly due to GAG accumulation may influence the biodistribution of IDUA, studies were performed in adult MPS I mice. The mice were injected with equimolar amounts of Tf-ID or Mono-ID plasmid, and enzyme levels were quantified in non-CNS and CNS tissues 48 hours later. In agreement with our previous data, Tf-ID exhibited high levels of extracellular enzyme (*i.e.*, in the serum), whereas Mono-ID showed high levels in the tissue of protein production (liver). In addition to being more effective in reaching the brain, the Tf-ID enzyme was also more effective than Mono-ID in accessing the gastrointestinal tract, kidney, and lung, as well as the treatment-refractory tissues of the heart and brain (Figure 5a).

In order to identify the cells in the CNS that acquired the Tf-ID protein, we performed immunofluorescence microscopy on brain sections of Tf-ID- and Mono-ID plasmid-injected mice. Figure 5b shows the cerebellum of an untreated MPS I mouse. Tf-ID-treated animals showed no staining when sections were incubated with rabbit preimmune sera (Figure 5c). Incubation of Mono-ID-treated animals (Figure 5d) with an anti-human IDUA antibody revealed no staining, whereas, in Tf-ID animals, cytoplasmic staining of Purkinje cells was evident (Figure 5e).

In order to assess the ability of Tf-ID to ameliorate GAG pathology, adult MPS I animals were treated with a single, equimolar dose of either Mono-ID or Tf-ID, and killed 3 weeks later. Visceral tissues and brain were removed and stained with Alcian blue, which stains GAGs. Both Mono-ID and Tf-ID produced GAG reduction in visceral tissues (not shown). In the choroid plexus and meninges of Mono-ID-treated and IDUA-knockout animals GAG accumulation was prevalent, whereas Tf-ID-treated animals showed reduction to near-normal levels (data not shown). Hematoxylin and eosin staining of the cerebellum showed vacuolation of all the Purkinje cells in untreated knockout animals and in those receiving Mono-ID (Figure 6a and b). Conversely, Tf-ID-treated animals showed clearance of some of the Purkinje cells (Figure 6c). Based on the detection of Tf-ID in the Purkinje cells by immunofluorescence and the observation of reduced vacuolation in these cells, we performed quantitative GAG analysis

in the cerebellums of untreated, Mono-ID- and Tf-ID-treated mice. We observed a significant reduction of cerebellar GAGs in Tf-ID-treated mice but not in the Mono-ID-treated animals (Figure 6d). These data indicate the potential of the Tf-ID fusion protein to reduce GAG accumulation from visceral tissues as well from the cerebellum.

## DISCUSSION

In this study, a fusion gene comprising Tf and human IDUA with an intervening 6-amino-acid linker was engineered. The N-terminal Tf motif maintained preferential specificity for the TfR, and the C-terminal IDUA maintained enzymatic activity and substrate specificity. The fusion protein showed proper targeting to the lysosome and, when delivered as plasmid DNA *in vivo*, resulted in high-level protein secretion into the blood. The resultant full-length Tf-ID, but not Mono-ID, protein was shown to enter the cytoplasm of cerebellar Purkinje cells of the brain and to reduce cerebellar GAG storage in adult MPS I mice.

The BBB is comprised of brain capillary endothelial cells that form a barrier through tight junctions, excluding the vast majority of large and small molecules.<sup>25</sup> Therefore, studies using recombinant IDUA have shown that it has little efficacy in relieving the lysosomal storage burden in the CNS. The TfR is expressed at the brain capillary endothelium and throughout the brain, and it has been targeted for transport of material into the CNS. Because lysosomal enzymes have shown themselves capable of functioning as fusion proteins<sup>18,26,27</sup> we hypothesized, and have now shown, that the generation of a TfR-targeted IDUA fusion gene results in a functional enzyme capable of TfR-mediated uptake with the potential of reducing CNS storage material.

Tf-ID was able to enter the CNS despite the potential for competition for the TfR from endogenous circulating Tf protein. Whereas physiological levels of Tf did not appear to inhibit uptake of the fusion protein into the CNS, supraphysiological levels of Tf did prevent Tf-ID uptake thereby indicating that a TfR-mediated uptake of Tf-ID was operative *in vivo* (Figure 4). Because the delivery of the Tf-ID-encoding plasmid *in vivo* results in continuous secretion of the fusion peptide, steady-state levels of enzyme are available to bind to the TfR even in the presence of endogenous Tf. Our studies extend those of Pardridge *et al.* who achieved TfR-mediated transport across the BBB using anti-TfR antibodies linked to a reporter enzyme,<sup>19</sup> and those of Bai<sup>28</sup> who demonstrated the transport of a cytokine from the intestinal lumen into the plasma, using an orally delivered cytokine-Tf fusion gene product.

Tf-ID uptake was inhibited *in vitro* and *in vivo* by addition of fTf, while addition of M6P resulted in only partial inhibition *in vitro* (Figure 2a). Given that the residues in IDUA which become mannose 6-phosphorylated have not been altered in our construct, it is not surprising that Tf-IDUA remains competent for partial M6PR-mediated uptake, thereby suggesting that a dual-uptake mechanism involving both TfR and M6PR may potentially be operative. Consistent with our studies, a dual-uptake mechanism has been reported for other “non-classically” targeted lysosomal fusion proteins. Uptake of an IDUA receptor-associated protein fusion in GM1391 fibroblasts was partially inhibited by the addition of free M6P, and completely inhibited by the addition of receptor-associated protein.<sup>26,27</sup>

We demonstrate that Tf-ID results in significantly higher serum IDUA levels as compared to Mono-ID on an equimolar basis of injected plasmid DNA, and that TfR-dependent uptake is the primary mechanism for access of Tf-ID into the CNS (Figure 4d and e). The specificity that Tf-ID shows for the TfR, coupled with the superior secretion of our enzyme as a result of the Tf secretion signal, may maximize the potential of this strategy to deliver therapeutic benefit in the CNS. High serum levels of enzyme have been associated with the amelioration of CNS pathology in MPS VII mice tolerogenic to the protein, as well as in immunosuppressed MPS I

mice treated with IDUA viral vectors.<sup>22,29</sup> In the latter instance, viral vectors may gain direct access to the CNS<sup>30,31</sup> or may be carried into the CNS by transduced hematopoietic cells that can form microglia.<sup>32</sup> This explanation does not appear to apply to our studies, as we were unable to detect plasmid DNA in the brain, at least not at the level of sensitivity of detection of bioluminescence from firefly luciferase activity. In the case of the tolerogenic MPS VII mice, the mechanism through which the enzyme accesses the brain is unknown. However, a recent study provides a possible explanation for this phenomenon. Urayama *et al.* show upregulation of the M6PR resulting from an injection of epinephrine, with concomitant transcytosis of  $\beta$ -glucuronidase across the BBB.<sup>33</sup> Because of the decline of M6PR associated with age,<sup>34</sup> the delivery of large doses of enzyme may be required to facilitate M6PR-mediated delivery to the brain in adult animals. This may hold true for the study conducted by Ma *et al.* as well.<sup>29</sup> These studies would indicate that lower enzyme levels may not have adequate access to the CNS because they fall below a critical threshold level, or may result in too small a biological effect on brain pathology to be detectable by the assays used. Whether this is true for all MPS diseases in animals as well as in humans is unknown, and warrants further investigation.

Studies in MPS I mice revealed that the expression of IDUA (Tf-ID and Mono-ID) peaked at 48 hours and then was gradually extinguished over a period of ~3 weeks (data not shown). This has been observed by others who have reported immune responses to the vector/transgene in MPS I mice, which hinder long-term expression in adult animals.<sup>29,35,36</sup> In MPS I mice, IDUA activity was abolished by 3 weeks after Tf-ID plasmid DNA injection. However, in nondepleted or natural killer-depleted SCID mice, enzyme activity remained slightly above endogenous levels and persisted at these levels for several more weeks (data not shown). While the relatively higher levels of IDUA in SCID mice as compared to MPS I mice are consistent with an immune response to IDUA in the latter,<sup>29,36</sup> the decrement in IDUA activity in SCID mice is consistent with transient expression from episomal DNA or heterochromatin formation on account of the plasmid back-bone, resulting in loss of transgene expression.<sup>37</sup> Nonetheless, the short-term expression we achieved in MPS I mice allowed for reduction of visceral and cerebellar storage material. GAG reduction in the meninges and choroid plexus, as well as absence of vacuolation in some Purkinje cells of Tf-ID was evident in histological examination. Importantly, quantitative biochemical GAG analysis showed a decrease in cerebellar GAGs in Tf-ID-treated mice but not in Mono-ID-treated mice (Figure 6d). Our immunofluorescence studies and pathology findings show the ability of Tf-ID to modulate the CNS pathology, including the Purkinje cells that are a major site of storage material in MPS I mice.<sup>38,39</sup>

In summary, we have shown that the *in vivo* hydrodynamic delivery of a Tf-ID plasmid resulted in production of a biologically active TfR-targeted protein in the liver, and that this protein gained access to the CNS of MPS I mice. Our data complement those of Spencer and Verma who demonstrated that the access of enzymes into the CNS could be achieved by delivering a glucocerebrosidase–low-density lipoprotein fusion construct, resulting in the presence of glucocerebrosidase in most of the Purkinje cells in the cerebellum.<sup>18</sup> While our studies demonstrate the ability of this strategy to modulate cerebellar GAG pathology, the ultimate goal will be to provide therapeutic benefit to all CNS areas affected by GAG accumulation. In order to ascertain the ability of our strategy to accomplish this, we have undertaken efforts to define the optimal gene delivery system that will allow for sustained gene expression, so that comprehensive neurological testing can be performed. Nevertheless, our findings represent a potential solution to one of the key challenges for the treatment of lysosomal storage disease, namely, CNS entry of systemically delivered enzyme.

## MATERIALS AND METHODS

### Plasmid construction

Murine Tf (including signal sequence and minus stop codon; nucleotides 1–2,091) was cloned from C57BL/6 liver RNA using reverse transcription-PCR, and inserted into the TOPO pcDNA3.1 D expression plasmid (Invitrogen, Carlsbad, CA). The forward primer was 5'-CACCATGAGGCTCACCGTGGGTGCCCTGC-3' and the reverse primer was 5'-TGTACCGGTTTCTGCCTCGGCATGTTTGTGGAAAGCGCAGGCTTC-3', which contained an *AgeI* restriction site in the linker region (underlined), creating space between Tf and IDUA. Human IDUA (kindly provided by Dr. Don Kohn, Los Angeles, CA) (minus signal sequence) was fused in-frame into the *AgeI* and *XhoI* sites using 5'-TGTACCGGTGAGGCCCGCACCTGGTGCAGGTGG-3' and 5'-TGTCTCGAGTCATGGATTGCCCGGGGATGGGGGCCCTCTTG-3'. Mono-ID plasmid was created by subcloning the full-length IDUA cDNA into pcDNA3.1. Removal of the signal sequence of Tf was accomplished by using 5'-TGTAAGCTTATGGTCCCTGACAAAACGGTCAAATGG-3' and the reverse primer described earlier. The product was digested with *HindIII* and *EcoRI* and inserted into the pcDNA3.1 vector to generate deltaSS Tf-ID. For recombinant protein production, a 6x histidine sequence termed Tf-IDUA 6xHis (polyhistidine is underlined in the reverse primer) was incorporated into the 3'-end of IDUA by PCR, using the Tf forward primer or a Mono-ID forward primer, the reverse primer being 5'-GACCGGTTCAATGGTGATGGTGATGTGGATTGCCCGGGGATG-3'. The Tf-ID-DsRed Fusion was created by removing the IDUA stop codon and adding an *AvrII* site into which the DsRed monomer was inserted (Clontech, Mountain View, CA), resulting in an in-frame Tf-ID-DsRM construct.

### *In vitro* assay of IDUA activity

IDUA activity was assessed using 4-methylumbelliferyl  $\alpha$ -L-iduronide as the substrate (NBS Biological, Corston, Bath, UK).<sup>40</sup> One million NIH-3T3 cells (American Type Culture Collection, Manassas, VA) were grown in triplicate in Dulbecco's modified Eagles medium/10% fetal bovine serum medium and nucleofected (Amaxa, Cologne, Germany) with equimolar amounts of Tf-IDUA or IDUA-alone plasmid (~5  $\mu$ g). Nucleofection conditions were program U-030/buffer R. IDUA activity was assessed at 48 hours in the supernatants of the cultures and in cellular lysates prepared in reporter lysis buffer (RLB; Promega, Madison, WI). Fluorescence was measured at an excitation level of 360 nm/emission 465 nm on a Chameleon plate reader (Bioscan, Washington DC). Protein concentration was determined using the Protein Quantification Kit—Wide Range (Dojindo, Gaithersburg, MD). Enzyme activity is defined in terms of units, one unit of enzyme being the amount that releases 1 nmol of 4-methylumbelliferone in 1 hour.<sup>41</sup>

### Cellular localization

Tf-ID-DsRM plasmid was nucleofected (Amaxa; Buffer T; Program U-23) into CHO-TRvB cells (a generous gift from Dr. H. Phillip Koeffler, Cedars-Sinai Medical Center, Los Angeles, CA) and plated on two-chamber polystyrene vessel tissue culture-treated glass slides (BD Falcon, San Jose, CA) for 24 hours. LysoTracker Green DND-26 (Invitrogen) was added for 30 minutes, and the cells were then washed, fixed in acetone, 4'-6-diamidino-2-phenylindole stained (Vector Laboratories, Burlingame, CA), and analyzed using an Olympus BX 51 fluorescent microscope (Leeds Precision Instruments, Minneapolis, MN).

### Recombinant Tf-IDUA isolation and uptake studies

Fifty microgram of Tf-IDUA6xHis was injected hydrodynamically into the lateral tail veins of NOD-SCID mice purchased from the Jackson Laboratories and housed at the University of Minnesota.<sup>21</sup> At 48 hours after the injection, sera were collected and pooled, before isolation using a HisTrap FF Crude Nickel-NTA Column (GE Healthcare, Piscataway, NJ). Enzyme was eluted off the column with 250 mmol/l imidazole in phosphate buffer. 100,000 3T3 cells were seeded in triplicate 24 hours prior to enzyme addition. One day after the seeding, endogenous Tf (Sigma-Aldrich, St. Louis, MO) was removed by incubating two times in serum-free medium [Hamm's F12 (Invitrogen)/0.5% bovine serum albumin (Sigma)] for 1 hour each time. Recombinant Tf-ID or recombinant human IDUA (Aldurazyme; Genzyme, Cambridge, MA) at an equal activity level was added to wells containing free M6P (1.5 mmol/l; Sigma), free bovine holo-Tf (fTf; 2.5 mg; Sigma), or neither, and incubated at 37 °C for 1 hour. The cells were washed on ice [phosphate-buffered saline (PBS)/0.2% bovine serum albumin], trypsinized, and lysed in RLB, and the IDUA assay was performed by overnight incubation at 37 °C with 4-methylumbelliferyl  $\alpha$ -L-iduronide and normalized to protein.

### Fusion protein activity and specificity for the TfR

Recombinant Tf-ID was isolated as described in the earlier text. Animals were also injected with Mono-ID6xHis so that comparative studies with each version of the enzyme could be performed on samples isolated in the same fashion. Western blot analysis was then carried out by loading samples on a NuPAGE 3–8% Tris–acetate gel, separating the samples using the XCell SureLock Mini-Cell, and transferring to an Invitrolon polyvinylidene difluoride membrane using the XCell II blot module (all from Invitrogen). Membranes were blocked in 3% milk-PBS and probed with either a polyclonal rabbit anti-Tf antibody (Abcam, Cambridge, MA) or the BP13BL2 rabbit anti-human IDUA antibody (kindly provided by Emil Kakkis, BioMarin Pharmaceutical, Novato, CA) at a concentration of 1:3,000 overnight at 4 °C. Horseradish peroxidase–conjugated goat anti-rabbit antibody (Abcam) was added at a ratio of 1:5,000, and enhanced chemiluminescence was performed using the ECL Plus western blotting detection System (GE Healthcare). Densitometry was then performed using a FluoroChem imaging system and version 3.1 software (Alpha Innotech, San Leandro, CA). Enzyme activity was determined using 4-methylumbelliferyl  $\alpha$ -L-iduronide as the substrate. Tf-ID activity was expressed as a percentage of the enzyme activity of Mono-ID, which was designated as 100%. For TfR affinity, 3T3 cells were depleted of endogenous Tf as detailed earlier. Either no inhibitor at all (control), or equimolar amounts of free Tf (Sigma) or recombinant Tf-ID protein (determined by quantitative western blot, performed as described earlier with known amounts of Aldurazyme as a standard) were incubated with the cells, followed by the addition of 1  $\mu$ g of a Tf-fluorescein isothiocyanate conjugate (Sigma) and incubation at 4 °C for 30 minutes with continuous agitation. The cells were washed three times with PBS, and fluorescence was measured at an excitation level of 485 nm/emission 530 nm (gain = 100) on a Chameleon plate reader (Bioscan, Washington DC). The percentage uptake for cells not receiving any inhibitor was designated as 100% (control). The uptake levels of free Tf and Tf-ID samples were expressed in relation to the control.

### *In vivo* studies in NOD-SCID (IDUA<sup>+/+</sup>) mice to measure activity in brain and serum

NOD-SCID mice were injected by hydrodynamic tail vein injection<sup>21</sup> with equimolar amounts of Tf-ID, Mono-ID, or deltaSS Tf-, and brain and serum were removed. Brain was lysed in RLB and IDUA levels were determined using 4-methylumbelliferyl  $\alpha$ -L-iduronide (1-hour incubation for serum and overnight incubation for brain, followed by normalization to protein).

Sera from the mice were analyzed using western blot as detailed in the earlier text.



### Biodistribution of plasmid DNA

Two hundred and fifty microgram of a cytomegalovirus-driven firefly luciferase plasmid (cloned into the Invitrogen pcDNA3.1 vector from the pGL vector from Promega) was injected into the tail veins of NOD-SCID mice. At 48 hours after the injection Xenogen imaging was performed as described.<sup>20</sup> The animals were killed, and the organs from each individual animal were removed and homogenized in RLB. *In vitro* assays were performed using the luciferase assay system (Promega) and read on the Chameleon plate reader (Bioscan).

### Brain capillary depletion

NOD-SCID mice were treated with 115 µg of Aldurazyme (Genzyme) or 10 µg of Tf-ID plasmid. One hour after the Aldurazyme injection and 48 hours after the Tf-ID injection the animals were killed, the brains were removed and weighed, and brain capillary depletion was carried out as described.<sup>19,23,34</sup> Note the difference in the y-axis in Figure 4 c and d. Because this procedure involves the use of dextran which binds the Bradford dye, we relied on brain weights determined by analytical scale for calculating the concentration.

### Uptake studies

Tf was provided as bovine Tf (Sigma) through intraperitoneal injections (5 mg) every 12 hours for 48 hours before the plasmid injection. Fifty micrograms of Tf-ID was injected into NOD-SCID animals, which then received intraperitoneal injections of Tf every 12 hours for an additional 48 hours, at which time point the animals were killed. Other animals received Tf-ID plasmid in the absence of inhibitor. Forty-eight hours after the plasmid injection, the sera of animals from all the groups were drawn. The animals were then killed, the jugular vein was severed, and transcardial perfusion with PBS was carried out. Brain lysates were prepared in RLB for IDUA activity as described in the earlier text.

### Enzyme biodistribution in MPS I mice

The IDUA<sup>-/-</sup> breeder mice used for establishing our colony were kindly provided by Dr. Lorne Clarke (University of British Columbia, Vancouver, Canada).<sup>38</sup> Equimolar amounts of Tf-ID or Mono-ID plasmids were injected into C57BL/6 IDUA<sup>-/-</sup> mice, and IDUA activity was quantified at 48 hours after the injection.

### Immunofluorescence

Untreated MPS I mice or MPS I mice treated with Mono-ID or Tf-ID by tail vein injection were killed at 48 hours after the injection, perfused with 4% paraformaldehyde, and embedded in optimal cutting temperature (Sakura Finetek, Torrance, CA). Sections of 4–6 µm were cut on a CM1900 Cryostat (Leica, Wetzlar, Germany) and fixed in acetone (Sigma). The sections were incubated with Background Sniper (Biocarta, San Diego, CA) for 12 minutes, rinsed with PBS, and stained overnight with either BP13 preimmune rabbit serum or the BP13BL2 antihuman IDUA antibody (BioMarin Pharmaceutical, Novato, CA) at a concentration of 1:3,000 at 4 °C. The slides were rinsed with PBS, stained with an anti-rabbit Cy3 antibody (Jackson ImmunoResearch, West Grove, PA) at 1:500 for 1 hour, stained with 4'-6-diamidino-2-phenylindole (Vector Laboratories, Burlingame, CA), cover slipped and analyzed using an Olympus BX51 fluorescent microscope (Leeds Precision Instruments).

### Pathology

IDUA mice were treated with equimolar amounts of Tf-ID or Mono-ID. Three weeks after the injection, the animals were killed and the tissues were removed. The brains were embedded in optimal cutting temperature, and 6-µm sections were cut as described earlier. The sections were stained with Alcian blue or hematoxylin and eosin.

## Quantitative GAG analysis

One hemisphere of the brain was utilized for quantitating GAGs in the cerebellum using the Blyscan GAG assay kit (Biocolor, Northern Ireland) followed by normalization to protein.

## ACKNOWLEDGMENTS

We thank R. Scott McIvor for helpful discussions and Andrew Price, Kevin Tram, and Christopher Lees for technical assistance. This work was supported by an award from the American Heart Association (to M.J.O.) and National Institutes of Health Grants R01 HL49997 and HL52952 (to B.R.B).

## REFERENCES

1. Neufeld, EF.; Muenzer, J. The mucopolysaccharidoses. In: Scriver, CR.; Beaudet, AL.; Sly, WS.; Valle, D., editors. *The Metabolic and Molecular Bases of Inherited Disease*. New York: McGraw-Hill; 2001. p. 3421-3452.
2. Hopwood JJ, Morris CP. The mucopolysaccharidoses. Diagnosis, molecular genetics and treatment. *Mol Biol Med* 1990;7:381–404. [PubMed: 2128891]
3. Fowler GW, Sukoff M, Hamilton A, Williams JP. Communicating hydrocephalus in children with genetic inborn errors of metabolism. *Childs Brain* 1975;1:251–254. [PubMed: 810326]
4. Kaufman HH, Rosenberg HS, Scott CI, Lee YY, Pruessner JL, Butler IJ. Cervical myelopathy due to dural compression in mucopolysaccharidosis. *Surg Neurol* 1982;17:404–410. [PubMed: 6810485]
5. Kennedy P, Swash M, Dean MF. Cervical cord compression in mucopolysaccharidosis. *Dev Med Child Neurol* 1973;15:194–199. [PubMed: 4266829]
6. Paulson GW, Meagher JN, Burkhart J. Spinal pachymeningitis secondary to mucopolysaccharidosis. Case report. *J Neurosurg* 1974;41:618–621. [PubMed: 4278439]
7. Robertson SP, Klug GL, Rogers JG. Cerebrospinal fluid shunts in the management of behavioural problems in Sanfilippo syndrome (MPS III). *Eur J Pediatr* 1998;157:653–655. [PubMed: 9727849]
8. Muenzer J. Mucopolysaccharidoses. *Adv Pediatr* 1986;33:269–302. [PubMed: 3099554]
9. Peters C, Balthazor M, Shapiro EG, King RJ, Kollman C, Hegland JD, et al. Outcome of unrelated donor bone marrow transplantation in 40 children with Hurler syndrome. *Blood* 1996;87:4894–4902. [PubMed: 8639864]
10. Kakkis ED. Enzyme replacement therapy for the mucopolysaccharide storage disorders. *Expert Opin Investig Drugs* 2002;11:675–685.
11. Kakkis ED, Muenzer J, Tiller GE, Waber L, Belmont J, Passage M, et al. Enzyme-replacement therapy in mucopolysaccharidosis I. *N Engl J Med* 2001;344:182–188. [PubMed: 11172140]
12. Krivit W, Sung JH, Shapiro EG, Lockman LA. Microglia: the effector cell for reconstitution of the central nervous system following bone marrow transplantation for lysosomal and peroxisomal storage diseases. *Cell Transplant* 1995;4:385–392. [PubMed: 7582569]
13. Kakkis E, McEntee M, Vogler C, Le S, Levy B, Belichenko P, et al. Intrathecal enzyme replacement therapy reduces lysosomal storage in the brain and meninges of the canine model of MPS I. *Mol Genet Metab* 2004;83:163–174. [PubMed: 15464431]
14. Thomas JA, Jacobs S, Kierstein J, Van Hove J. Outcome after three years of laronidase enzyme replacement therapy in a patient with Hurler syndrome. *J Inherit Metab Dis* 2006;29:762. [PubMed: 17089217]
15. Tokic V, Barisic I, Huzjak N, Petkovic G, Fumic K, Paschke E. Enzyme replacement therapy in two patients with an advanced severe (Hurler) phenotype of mucopolysaccharidosis I. *Eur J Pediatr* 2006;166:727–732. [PubMed: 17043838]
16. Kroll RA, Neuwelt EA. Outwitting the blood-brain barrier for therapeutic purposes: osmotic opening and other means. *Neurosurgery* 1998;42:1083–1099. [PubMed: 9588554]discussion 1099–1100.
17. Pardridge WM. The blood-brain barrier: bottleneck in brain drug development. *NeuroRx* 2005;2:3–14. [PubMed: 15717053]
18. Spencer BJ, Verma IM. Targeted delivery of proteins across the blood-brain barrier. *Proc Natl Acad Sci USA* 2007;104:7594–7599. [PubMed: 17463083]

19. Zhang Y, Pardridge WM. Delivery of  $\beta$ -galactosidase to mouse brain via the blood-brain barrier transferrin receptor. *J Pharmacol Exp Ther* 2005;313:1075–1081. [PubMed: 15718287]
20. Osborn MJ, Panoskaltis-Mortari A, McElmurry RT, Bell SK, Vignali DA, Ryan MD, et al. A picornaviral 2A-like sequence-based tricistronic vector allowing for high-level therapeutic gene expression coupled to a dual-reporter system. *Mol Ther* 2005;12:569–574. [PubMed: 15964244]
21. Zhang G, Budker V, Wolff JA. High levels of foreign gene expression in hepatocytes after tail vein injections of naked plasmid DNA. *Hum Gene Ther* 1999;10:1735–1737. [PubMed: 10428218]
22. Vogler C, Levy B, Grubb JH, Galvin N, Tan Y, Kakkis E, et al. Overcoming the blood-brain barrier with high-dose enzyme replacement therapy in murine mucopolysaccharidosis VII. *Proc Natl Acad Sci USA* 2005;102:14777–14782. [PubMed: 16162667]
23. Triguero D, Buciak J, Pardridge WM. Capillary depletion method for quantification of blood-brain barrier transport of circulating peptides and plasma proteins. *J Neurochem* 1990;54:1882–1888. [PubMed: 2338547]
24. Wraith JE, Clarke LA, Beck M, Kolodny EH, Pastores GM, Muenzer J, et al. Enzyme replacement therapy for mucopolysaccharidosis I: a randomized, double-blinded, placebo-controlled, multinational study of recombinant human  $\alpha$ -L-iduronidase (aronidase). *J Pediatr* 2004;144:581–588. [PubMed: 15126990]
25. Ueno M. Molecular anatomy of the brain endothelial barrier: an overview of the distributional features. *Curr Med Chem* 2007;14:1199–1206. [PubMed: 17504140]
26. LeBowitz JH, Grubb JH, Maga JA, Schmiel DH, Vogler C, Sly WS. Glycosylation-independent targeting enhances enzyme delivery to lysosomes and decreases storage in mucopolysaccharidosis type VII mice. *Proc Natl Acad Sci USA* 2004;101:3083–3088. [PubMed: 14976248]
27. Prince WS, McCormick LM, Wendt DJ, Fitzpatrick PA, Schwartz KL, Aguilera AI, et al. Lipoprotein receptor binding, cellular uptake, and lysosomal delivery of fusions between the receptor-associated protein (RAP) and  $\alpha$ -L-iduronidase or acid  $\alpha$ -glucosidase. *J Biol Chem* 2004;279:35037–35046. [PubMed: 15170390]
28. Bai Y, Ann DK, Shen WC. Recombinant granulocyte colony-stimulating factor-transferrin fusion protein as an oral myelopoietic agent. *Proc Natl Acad Sci USA* 2005;102:7292–7296. [PubMed: 15870205]
29. Ma X, Liu Y, Tittiger M, Hennig A, Kovacs A, Popelka S, et al. Improvements in mucopolysaccharidosis I mice after adult retroviral vector-mediated gene therapy with immunomodulation. *Mol Ther* 2007;15:889–902. [PubMed: 17311010]
30. Gonin P, Gaillard C. Gene transfer vector biodistribution: pivotal safety studies in clinical gene therapy development. *Gene Ther* 2004;11:S98–S108. [PubMed: 15454964]
31. Pan D, Gunther R, Duan W, Wendell S, Kaemmerer W, Kafri T, et al. Biodistribution and toxicity studies of VSVG-pseudotyped lentiviral vector after intravenous administration in mice with the observation of *in vivo* transduction of bone marrow. *Mol Ther* 2002;6:19–29. [PubMed: 12095299]
32. Biffi A, Naldini L. Gene therapy of storage disorders by retroviral and lentiviral vectors. *Hum Gene Ther* 2005;16:1133–1142. [PubMed: 16218774]
33. Urayama A, Grubb JH, Banks WA, Sly WS. Epinephrine enhances lysosomal enzyme delivery across the blood brain barrier by up-regulation of the mannose 6-phosphate receptor. *Proc Natl Acad Sci USA* 2007;104:12873–12878. [PubMed: 17646643]
34. Urayama A, Grubb JH, Sly WS, Banks WA. Developmentally regulated mannose 6-phosphate receptor-mediated transport of a lysosomal enzyme across the blood-brain barrier. *Proc Natl Acad Sci USA* 2004;101:12658–12663. [PubMed: 15314220]
35. Di Domenico C, Di Napoli D, Gonzalez Y, Reyero E, Lombardo A, Naldini L, Di Natale P. Limited transgene immune response and long-term expression of human  $\alpha$ -L-iduronidase in young adult mice with mucopolysaccharidosis type I by liver-directed gene therapy. *Hum Gene Ther* 2006;17:1112–1121. [PubMed: 17044753]
36. Aronovich EL, Bell JB, Belur LR, Gunther R, Koniar B, Erickson DC, et al. Prolonged expression of a lysosomal enzyme in mouse liver after Sleeping Beauty transposon-mediated gene delivery: implications for non-viral gene therapy of mucopolysaccharidoses. *J Gene Med* 2007;9:403–415. [PubMed: 17407189]

37. Chen ZY, Riu E, He CY, Xu H, Kay MA. Silencing of episomal transgene expression in liver by plasmid bacterial backbone DNA is independent of CpG methylation. *Mol Ther* 2008;16:548–556. [PubMed: 18253155]
38. Clarke LA, Russell CS, Pownall S, Warrington CL, Borowski A, Dimmick JE, et al. Murine mucopolysaccharidosis type I: targeted disruption of the murine  $\alpha$ -l-iduronidase gene. *Hum Mol Genet* 1997;6:503–511. [PubMed: 9097952]
39. Watson G, Bastacky J, Belichenko P, Buddhikot M, Jungles S, Vellard M, et al. Intrathecal administration of AAV vectors for the treatment of lysosomal storage in the brains of MPS I mice. *Gene Ther* 2006;13:917–925. [PubMed: 16482204]
40. Hopwood JJ, Muller V, Smithson A, Baggett N. A fluorometric assay using 4-methylumbelliferyl  $\alpha$ -l-iduronide for the estimation of  $\alpha$ -l-iduronidase activity and the detection of Hurler and Scheie syndromes. *Clin Chim Acta* 1979;92:257–265. [PubMed: 114339]
41. Liu Y, Xu L, Hennig AK, Kovacs A, Fu A, Chung S, et al. Liver-directed neonatal gene therapy prevents cardiac, bone, ear, and eye disease in mucopolysaccharidosis I mice. *Mol Ther* 2005;11:35–47. [PubMed: 15585404]

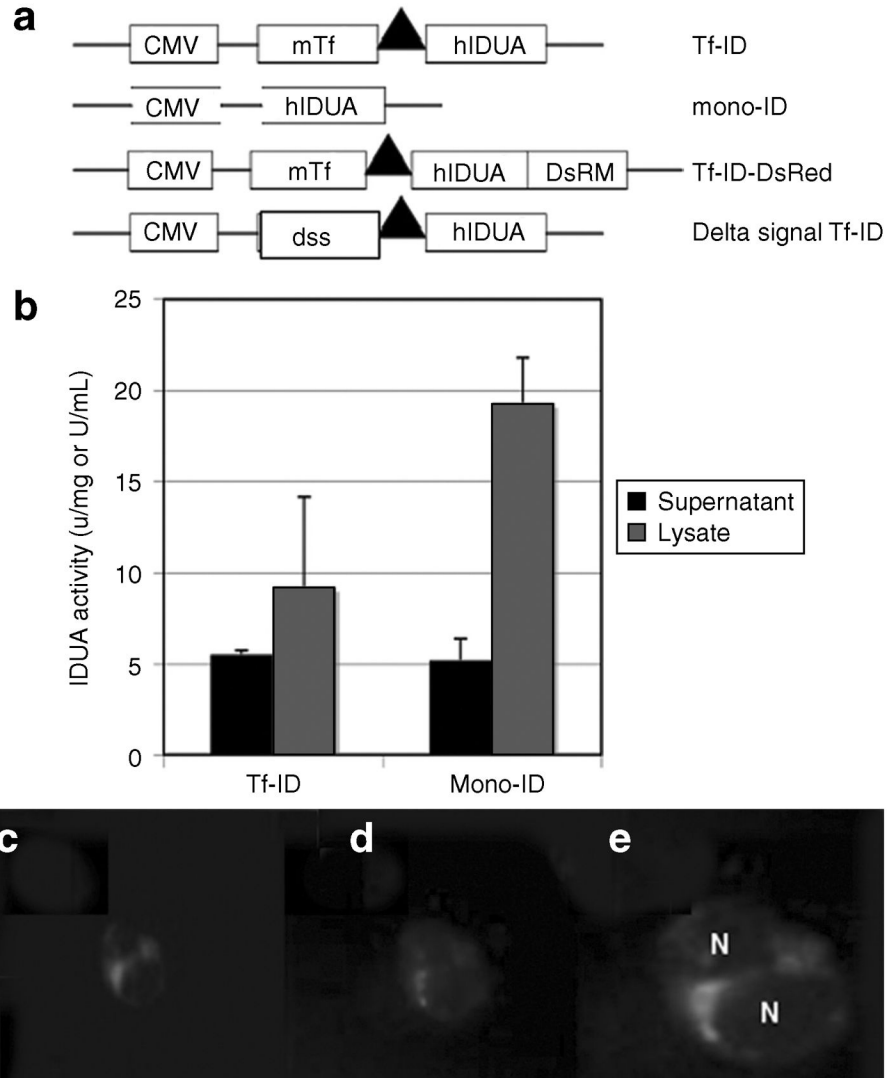


**Figure 1. Plasmid constructs, cellular localization, and activity**

(a) Top to bottom: cytomegalovirus (CMV) promoter-driven murine transferrin (Tf) fused to human  $\alpha$ -L-iduronidase (IDUA) (Tf-ID) with a 6-amino-acid linker (triangle); full-length human IDUA (Mono-ID); Tf-ID fused to the DsRed monomer red fluorescent protein; Tf-ID devoid of Tf signal sequence. Plasmid activity *in vitro*. (b) NIH-3T3 cells were nucleofected with Tf-ID or Mono-ID. IDUA activity was quantified in the cultured supernatant (U/ml) and cellular lysates (U/mg of total protein). Cellular localization. (c) Chinese hamster ovary cells were transfected with Tf-ID fused to DsRed monomer, and then (d) LysoTracker Green was added. (e) Merged image of c and d. N, cell nucleus. Scale bar, 10  $\mu$ m. Mean + SEM from triplicate samples are shown.

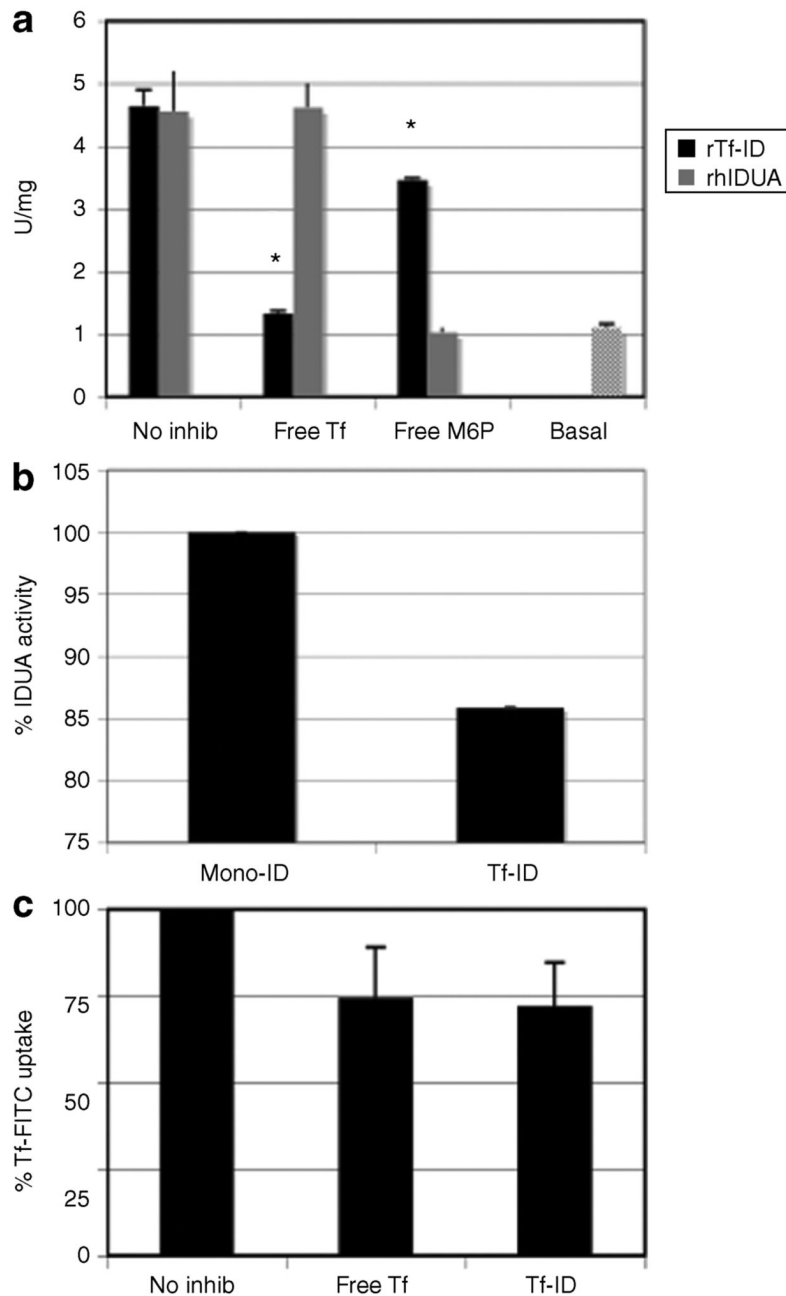


**Figure 2. Fusion protein uptake, activity, and specificity for the transferrin receptor (TfR)**

(a) Fusion protein uptake. NIH-3T3 cells were incubated with recombinant Tf-ID or recombinant  $\alpha$ -L-iduronidase (IDUA) (Aldurazyme) in the presence or absence of free Tf (fTf) or free mannose 6-phosphate (M6P). IDUA activity was quantified in cellular lysates. Basal refers to baseline 3T3 IDUA activity;  $P \leq .05$ . (b) Enzyme activity. Equimolar amounts of recombinant Tf-IDUA (rTf-IDUA) and Mono-ID were assessed for enzymatic activity. Mono-ID activity was designated as 100% and Tf-ID activity was compared against this value. (c) Specificity for the TfR. 3T3 cells were incubated with Tf conjugated to fluorescein isothiocyanate (FITC), either in the absence of any inhibitor or with equimolar amounts of fTf or recombinant Tf-ID. Tf-FITC in the absence of inhibitor was designated as 100% uptake.

Tf-FITC uptake values in the presence of fTf or Tf-ID were compared against this value. Mean values + SEM from triplicate samples are shown.

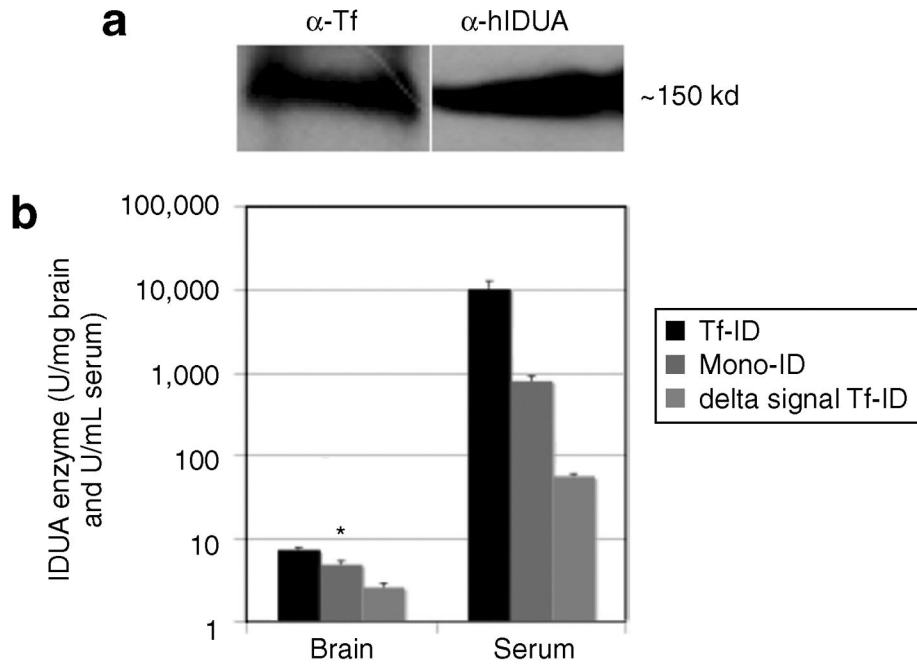


**Figure 3. *In vivo* study of Tf-ID fusion gene activity**

(a) Fusion protein western blot. Sera from Tf-ID-treated mice were subjected to a western blot and probed with anti-transferrin ( $\alpha$ -Tf) or anti-human  $\alpha$ -L-iduronidase (IDUA) antibodies (endogenous serum Tf band is not shown). (b) Tf-ID enzyme levels in the serum and brain were assessed after hydrodynamic tail vein injection of equimolar amounts of Tf-ID. Mono-ID, or deltaSS Tf-ID plasmid into nonobese diabetic-severe combined immunodeficiency mice ( $n = 5$  for Tf-ID and Mono-ID and  $n = 3$  for deltaSS Tf-ID). Mean + SEM are shown. Student's  $t$ -test (at 48 hours) \* $P = \leq 0.02$  for Tf-ID versus Mono-ID activity in brain. hIDUA, human IDUA.



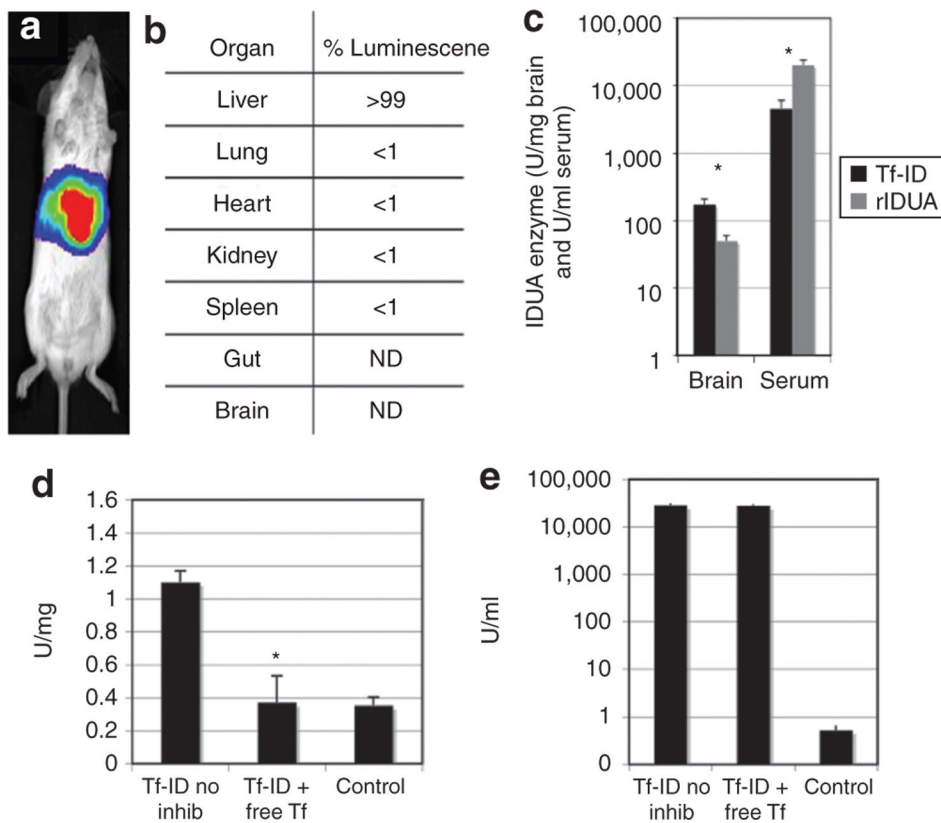


**Figure 4. Plasmid biodistribution, brain capillary depletion, and *in vivo* transferrin receptor blockade**

(a) Two animals were each injected with 250  $\mu$ g of a luciferase plasmid, and a representative bioluminescent image demonstrating gene expression in the liver is shown. (b) Organs from each animal were removed and the luminescence values from each organ were determined. The percentage of organ luminescence was determined by dividing the value for each individual organ by the total luminescence from all organs. (c) Animals were injected with either 115  $\mu$ g of Aldurazyme ( $n = 3$ ) or Tf-ID plasmid ( $n = 4$ ), and this was followed by serum and brain capillary depletion to determine  $\alpha$ -L-iduronidase (IDUA) activity. Mean + SEM are shown. Student's *t*-test:  $*P \leq 0.05$  for Aldurazyme versus Tf-ID in serum and for Tf-ID versus Aldurazyme in brain. (d) Tf-ID plasmid in the absence ( $n = 8$ ) or presence ( $n = 7$ ) of exogenous Tf was injected into nonobese diabetic-severe combined immunodeficiency mice, and brain IDUA activity was quantified at 48 hours after the injection. For comparison, the data from untreated controls ( $n = 4$ ) are shown. (e) Serum IDUA levels in animals referred to in d. Mean + SEM for each group are shown. Student's *t*-test:  $*P \leq 0.01$ . ND, no luciferase detected; rIDUA, recombinant IDUA; Tf, transferrin.

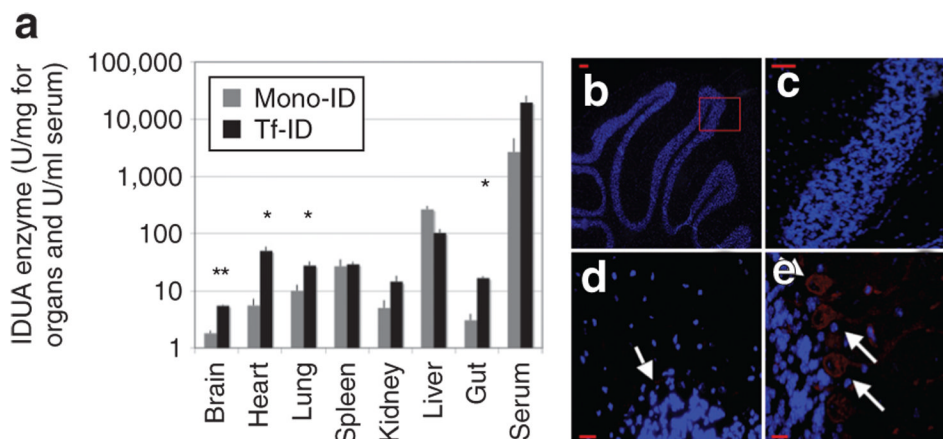


**Figure 5. *In vivo* biodistribution in mucopolysaccharidose type I (MPs I) mice, and tissue staining** (a) *In vivo* biodistribution of Tf-ID and Mono-ID in MPS I mice. Equimolar amounts of Tf-IDUA or Mono-ID plasmid were injected into MPS I mice, and the animals were killed and the tissues removed after 48 hours. IDUA levels were assessed in each tissue of the Tf-ID-treated animals ( $n = 4$ ) and the Mono-ID-treated animals ( $n = 3$ ). Mean + SEM for each group are shown. Student's  $t$ -test (at 48 hours): \*\* $P \leq 0.01$ , \* $P \leq 0.05$ . Tissue staining. MPS I (IDUA<sup>-/-</sup>) mice ( $n = 2$  each) were treated with either Tf-ID or Mono-ID plasmid, and immunofluorescence was performed after 48 hours. (b) Untreated animal, low magnification image of cerebellum. Scale bar is 100  $\mu$ m. The square represents the region shown in subsequent higher magnification images. (c) Tissue from Tf-IDUA-treated mouse, stained with preimmune rabbit serum, showing no background staining ( $\times 20$  magnification; scale bar is 50  $\mu$ m). (d) Tissue from Mono-IDUA-treated mouse, stained with BP13BL2 anti-IDUA antibody, showing no staining ( $\times 40$ ). (e) BP13BL2 antibody staining of tissues from Tf-IDUA-treated animal. White arrows show staining of the Purkinje cells in the cerebellum ( $\times 40$  magnification; scale bar is 10  $\mu$ m). IDUA,  $\alpha$ -L-iduronidase; Tf, transferrin.

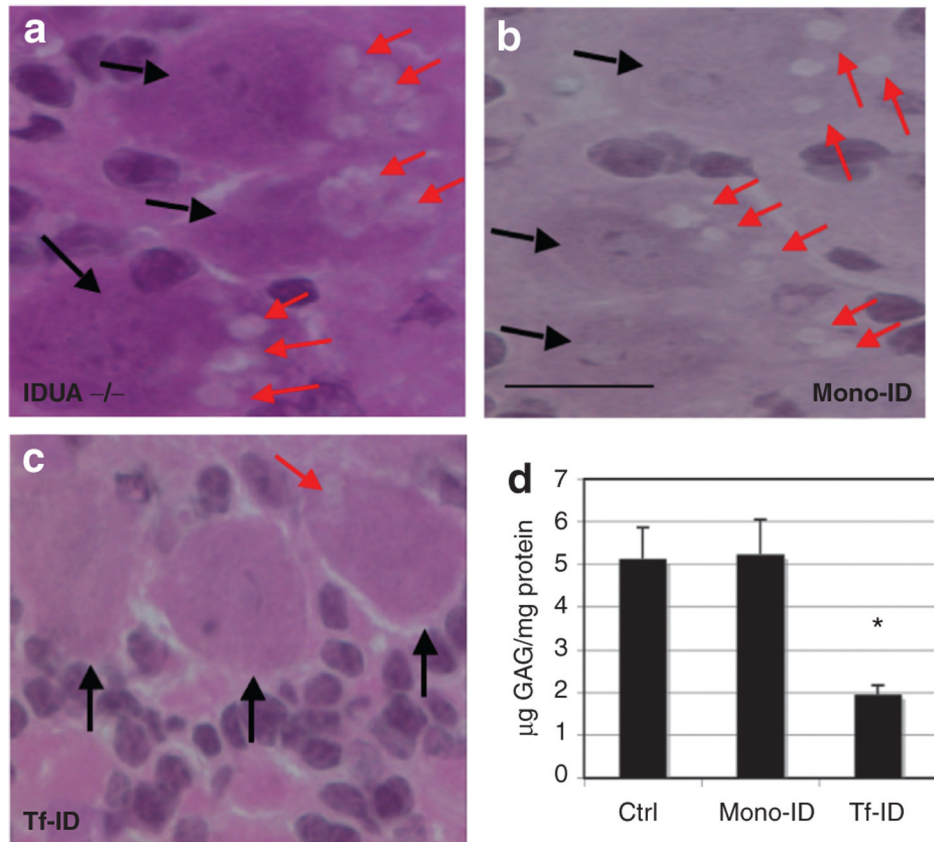


**Figure 6. Reduction in central nervous system pathology in mucopolysaccharidose type I (MPS I) mice**

Either Tf-ID or Mono-ID plasmid was administered to adult MPS I animals, and they were killed 3 weeks later. (a) Hematoxylin and eosin of Purkinje cell layer of untreated IDUA<sup>-/-</sup>, and (b) Mono-IDUA-treated mice. Black arrows show Purkinje cells. Red arrows show cytoplasmic vacuoles. (c) Tf-ID-treated mouse showing clearance of some Purkinje cells (black arrows). Vacuolated cells, decreased in number but still present (red arrows). Scale bar is 10 µm. (d) Quantitative glycosaminoglycan (GAG) analysis of cerebellum of IDUA<sup>-/-</sup>, Mono-ID-, and Tf-ID-treated mice ( $n = 3$  for each group). Student's  $t$ -test: \* $P \leq 0.02$ . Ctrl, control; IDUA,  $\alpha$ -L-iduronidase; Tf, transferrin.